EVALUATION OF WAVEFORM MAPPING AS A SIGNAL PROCESSING TOOL FOR QUANTITATIVE ULTRASONIC NDE

Patrick H. Johnston
NASA Langley Research Center
Hampton, Virginia

Doron Kishoni
College of William and Mary
Williamsburg, VA

INTRODUCTION

The mapping of one pulsed waveform into another, more desirable waveform by the application of a time-domain filter has been employed in a number of NDE situations [1-3]. The primary goal of these applications has been to improve the range resolution of an ultrasonic signal for detection of echoes arising from particular interfaces masked by the response of the transducer. The work presented here addresses the use of this technique for resolution enhancement in imaging situations and in mapping signals from different transducers to a common target waveform, allowing maintenance of quantitative calibration of ultrasonic systems. We also describe the use of this technique in terms of the frequency analysis of the resulting waveforms.

WAVEFORM MAPPING

The derivation of the waveform mapping algorithm has been fully described elsewhere [1]. A brief description is given here.

Considering a digitized RF pulse a_t and a desired RF pulse d_t, an operator f_t is sought that maps a_t into d_t, i.e. such that

$$a_t * f_t = d_t \tag{1}$$

Review of Progress in Quantitative Nondestructive Evaluation, Vol. 12
Edited by D.O. Thompson and D.E. Chimenti, Plenum Press, New York, 1993

where * denotes convolution. Because f_t cannot practically be defined to infinite length, the filter must be truncated to a finite length, which introduces errors. The truncated filter f'_t maps a_t into q_t, which is not identical to the desired signal:

$$a_t * f'_t = q_t \neq d_t. \tag{2}$$

The problem is approached by seeking the coefficients f'_t that yield least mean squared error between q_t and d_t.

The mean squared error E is defined according to

$$E = \sum_{t=0}^{\infty} (d_t - q_t)^2 \tag{3}$$

and it is minimized with respect to the filter coefficients f_t (dropping the prime for convenience)

$$\frac{\partial E}{\partial f_j} = \sum_{t=0}^{m+n} 2 \left(d_t - \sum_{s=0}^{m} f_s \, a_{t-s} \right) (a_{t-j}) = 0 \tag{4}$$

to obtain

$$\sum f_s \, r_{j-s} = g_j \tag{5}$$

where

$$r_{j-s} = \sum_{t=0}^{m+n} a_{t-s} \, a_{t-j} \tag{6}$$

is the autocorrelation of a_t and

$$g_j = \sum_{t=0}^{m+n} d_t \, a_{t-j} \tag{7}$$

is the cross correlation of a_t with the desired target d_t. The unknown filter coefficients f_t may be easily obtained using straightforward matrix techniques.

Now, this filter may be applied to achieve mapping with any other linear signal which is generated by convolution of a_t with another system response. For example, if

$$s_t = a_t * h_t, \tag{8}$$

then

$$f_t * s_t = f_t * (a_t * h_t) = (f_t * a_t) * h_t = q_t * h_t. \tag{9}$$

The signal has been converted into a convolution of the system response h_t with the waveform-mapped pulse q_t.

APPLICATION - STANDARDIZATION

The system impulse response of an ultrasonic NDE system can vary because of changes in settings or setup, aging or failure of transducers and electrical components, or swap-out of transducers or components. Thus, the pulse waveform generated by system may be different from day to day, setup to setup. Without careful calibration procedures, such variations may somewhat compromise the quantitative character of the data acquired with the system. Waveform mapping may be employed to standardize the data and allow continued quantitative assessment.

The measurement s_t can be described as the convolution of the measurement system impulse response A_t (transducer and electronics) with the impulse response h_t of the specimen under test

$$s_t = A_t * h_t. \tag{10}$$

Following some modification of the system, the system impulse response is now different, denoted as B_t. A filter $B\ A_t$ may be defined in which the new system response B_t is the input and the original system response A_t is the target

$$A_t = B\ A_t * B_t \tag{11}$$

and this filter may be applied to data acquired by the new system to map its response into that of the original system configuration

$$B\_A_t * (B_t * h_t) = (B\_A_t * B_t) * h_t = A_t * h_t \tag{12}$$

making the result comparable to data acquired with A_t.

To illustrate this, Fig. 1A presents two waveforms, one generated by driving a 5 MHz broadband transducer with a single cycle of 5 MHz andthe other generated by driving the same transducer with a single cycle of 8 MHz. This represents a relatively extreme case of differences between two similar systems. A waveform mapping filter was computed to map each of these waveforms to a target waveform derived form the 8 MHz signal. The resulting mapped pulses are plotted in Fig. 1B. Excellent agreement is observed between the two.

Another example is presented in Fig. 2. In Fig. 2A, four waveforms are plotted which represent data taken with the same transducer under different electronic damping conditions, such as may occur due to readjustment, modification, or replacement of the pulser/receiver circuitry. A target pulse was derived from one of the pulses, and each of the four waveforms were mapped to it. The resultant waveforms are presented in Fig. 2B. Again, the mapped waveforms agree very well.

APPLICATION - RESOLUTION IMPROVEMENT

As an illustration of the use of waveform mapping in an imaging system, a resolution target was constructed, patterned after resolution phantoms employed for medical

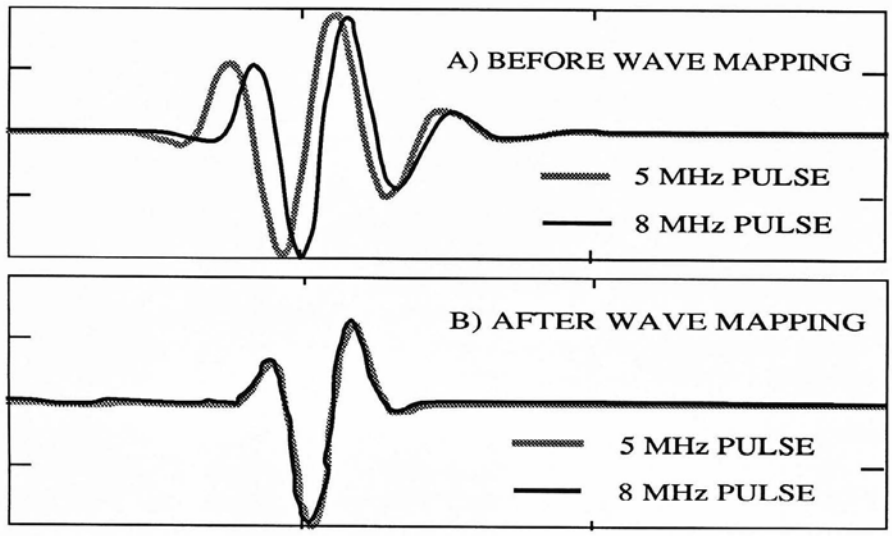

Fig. 1. Demonstration of standardization via wave mapping. A) Two waveforms before application of wave mapping. B) Same two waveforms after being mapped to the same target pulse.

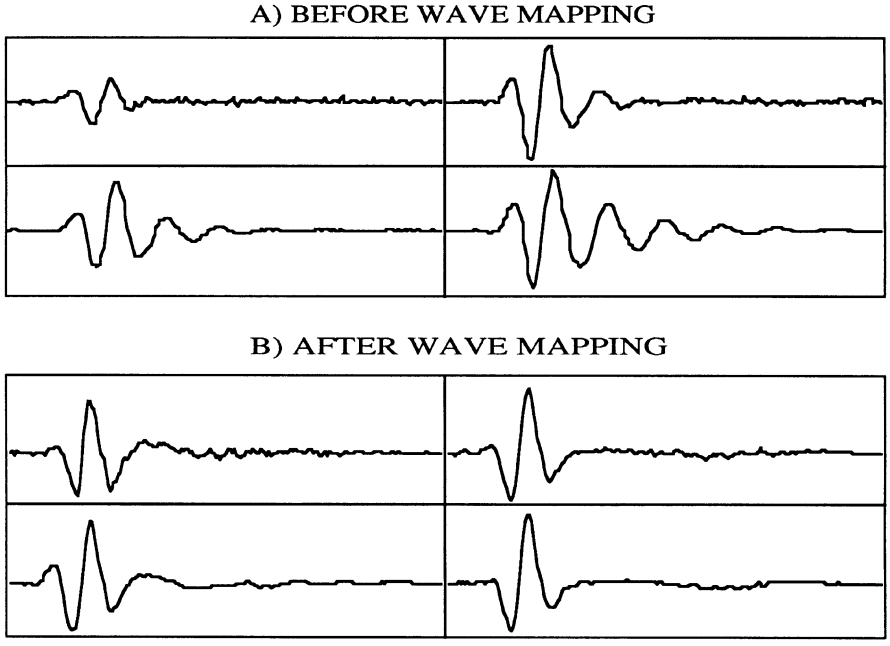

Fig. 2. Second example of standardiation via waveform mapping. A) Four waveforms produced by the same transducer, but with different damping. B) Same four waveforms after mapping them to a common target waveform.

ultrasonic imagers. A sketch of the phantom is shown in Fig. 3, along with the geometry of the ultrasonic data acquisition. The phantom consisted of monofilament fishing line (approximately 0.5 mm diameter) stretched between two plexiglas plates. The lines were spaced as shown in Fig. 3, with equal spacing in the lateral dimension and incrementally increasing spacing in the vertical dimension. The left hand panel indicates the geometry under which the B-scan was taken.

The echo waveform from the upper left target interrogated by a 5 MHz pulse is presented in Fig. 4A. Because the diameter of the target is between one and two wavelengths in water, the scattered echo is rather detailed, exhibiting several distinct pulses. An imaging system may be intended to indicate the target as a single pulse. To approach this result, a desired target pulse was derived from the initial wave packet in the signal, and a filter was computed to map the complex echo train into the single-pulse target waveform. A filter length of 256 coefficients was employed to achieve the goal, and the resulting waveform is plotted in Fig. 4B. The result is an excellent replica of the target, and the complexity of the scattering from the cylindrical target is removed to eneble clear imaging of the wire.

B-scan images of the wire targets are shown in Fig. 5. Fig. 5A is the amplitude B-scan of the target without waveform mapping applied. Each of the target echoes has a lateral dimension corresponding to the width of the ultrasonic beam, and the multi-peaked range signature is evident in the vertical dimension. The image presented in Fig. 5B is the result obtained after waveform mapping the same signals which were used to generate Fig. 5A. The signature of the upper left target, from which the filter was derived, has become a single line in the image. The vertical resolution of the image has been greatly enhanced,

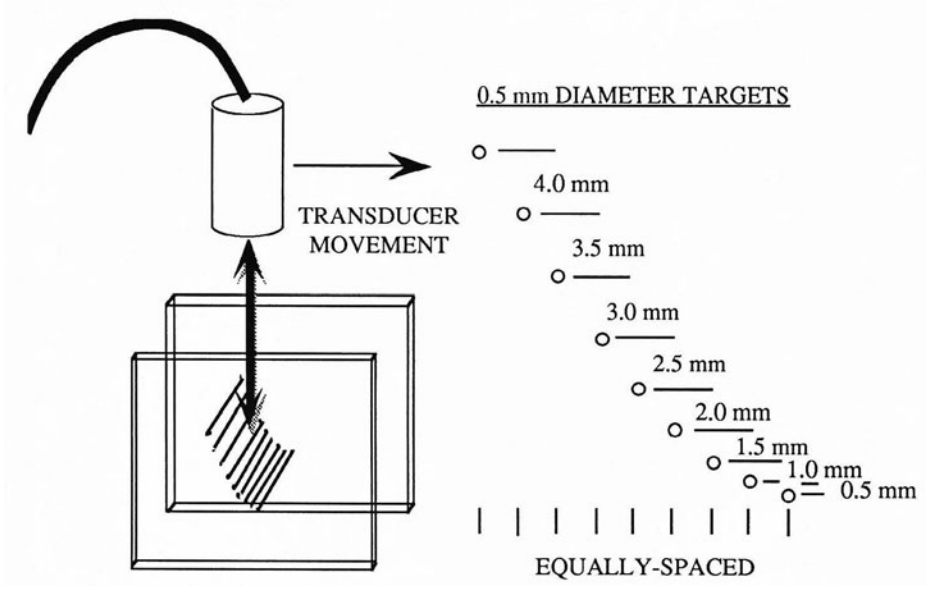

Fig. 3. Phantom for demonstration of range resolution enhancement via waveform mapping. Diagram on left shows the geometry of scanning for data acquisition. Diagram on the right shows the geometrical arrangement of the wire targets in the phantom.

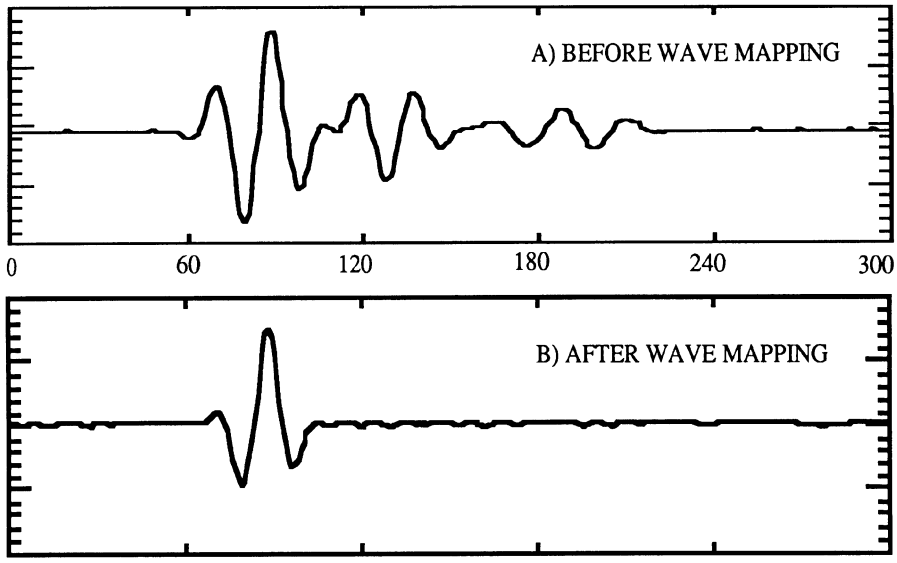

Fig. 4. A) Echo from a single target in the phantom. Backscattered waveform is complicated because the target has dimension on the order of a wavelength. B) Result of waveform mapping the signal from A above.

even at the lower portion of the phantom where errors due to diffraction effects are most evident. Derivation of the waveform mapping filter from a target near the center of the image region would be expected to result in more uniform resolution improvement over the image.

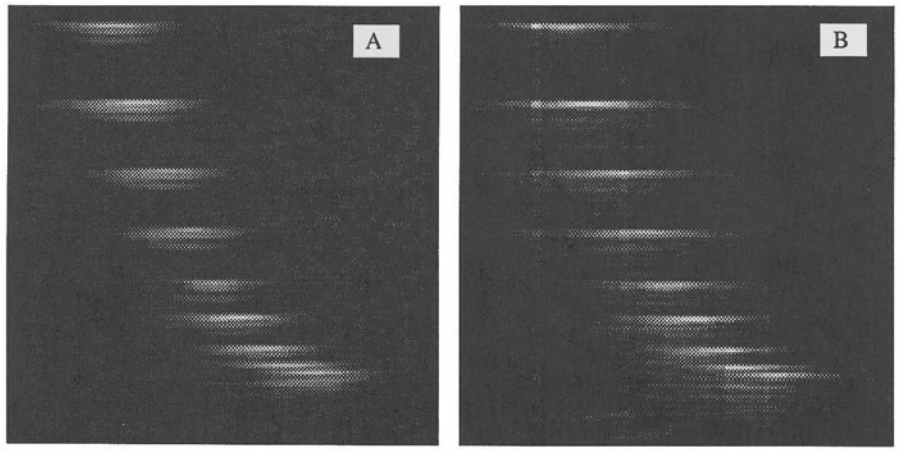

Fig. 5. B-scan images of the phantom. A) B-scan made from waveforms as measured. Each target has lateral dimension determined by beam width, and range signature determined by the complicated scattering waveform (Fig. 4A). B) B-scan made from same data after waveform mapping, using a filter derived to sharpen the upper left target (Fig 4B).

SPECTRAL CONSIDERATIONS

The process of waveform mapping is a linear filtering process, so that one way to view the process is in terms of the passband characteristics of the filter. Considerations of this type can be very useful in determining parameters of the filter.

Fig. 6 presents an echo waveform from the wire resolution phantom along with a target waveform and a number of filters, each with a different number of coefficients, designed to map between the two. In this case, where the input waveform is of relatively high complexity and duration, it is expected that the shorter filters cannot perform the mapping very well, as they do not span the duration of the details in the input waveform. By inspection, it is anticipated that a filter of 128 points would be the minimum expected to closely map the input into the target.

The filters are presented in the frequency domain in Fig. 7. The spectral ratio between the input waveform and the target waveform, which represents the target filter passband, is shown as the bottom-most curve. The passband for each filter was obtained by zero-padding to 256 points and applying a Fourier transform. The filter magnitudes are plotted with vertical offsets to allow comparison of their shapes without excessive overlapping.

It can be seen that while the 16-point filter completely misses the target shape, the 32-point filter has captured the gross shape of the target filter passband. Comparison of the filter functions in Fig. 6 shows that the 32-point filter shape remains nearly unchanged in the beginning of each of the longer filters. The 128-point filter begins to show the more rapid fluctuations in the spectrum, and the 256-point result is nearly perfect.

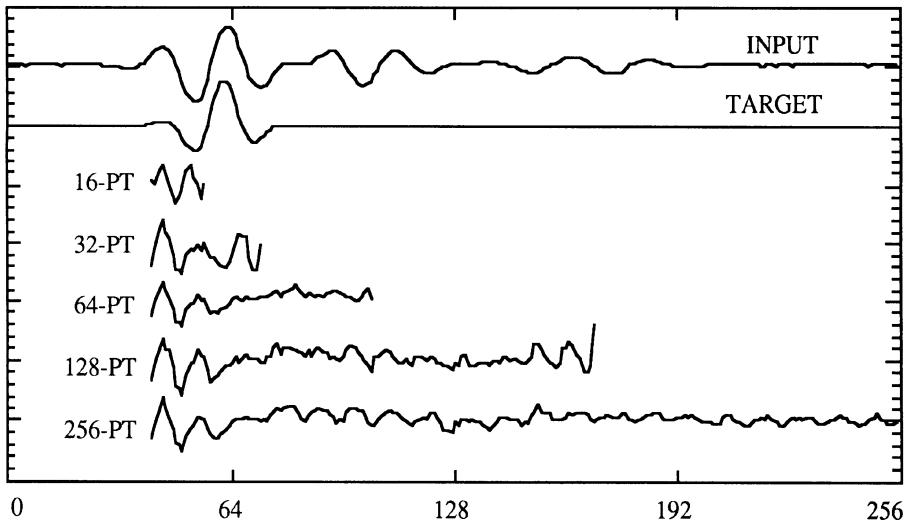

Fig. 6. Echo from a single target in the phantom, a target pulse derived from the initial portion of the signal, and a number of waveform mapping filters, each with a different number of coefficients, designed to map the echo into the target pulse.

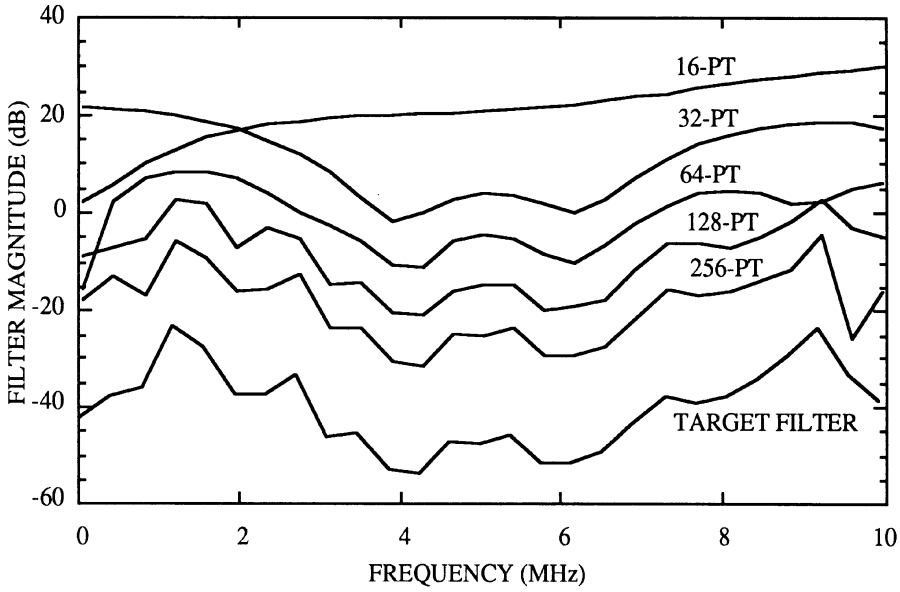

Fig. 7. Spectral presentation of waveform mapping filters. The target filter spectrum is the desired passband. The other curves represent the spectral magnitude of each of the filters in Fig. 6, padded to 256 points before transforming.

CONCLUSION

In this paper, waveform mapping for standardization of transducer signals and for range resolution enhancement has been demonstrated. It is believed that this method has considerable usefulness for ultrasonics and other pulsed systems. Work is continuing to evaluate the limitations and scope of the method, and to develop methods for optimizing target waveforms in particular applications.

REFERENCES

1. D. Kishoni, in *Review of Progress in Quantitative NDE*, Vol. 5A, edited by D.O. Thompson and D.E. Chimenti (Plenum Press, New York, 1985), pp. 781-787.

2. P.H. Johnston and D. Kishoni, in *Review of Progress in Quantitative NDE*, Vol. 7B, edited by D.O. Thompson and D.E. Chimenti (Plenum Press, New York, 1987), pp. 995-1001.

3. D. Kishoni, Invited, in *NATO Advanced Research Workshop (ARW 166/87) on Signal Processing and Pattern Recognition in Nondestructive Evaluation of Materials*, Lac Beauport, Quebec, Canada (August 19-22, 1987), edited by C. H. Chen (Springer-Verlag, Berlin Heidelberg 1988), NATO ASI Series, Vol. F44, pp. 117-127.